

Bitcoin Under Stress: Measuring Infrastructure Resilience 2014–2025

Wenbin Wu

Cambridge Centre for Alternative Finance
Cambridge, UK
w.wu@jbs.cam.ac.uk

Alexander Neumueller

Cambridge Centre for Alternative Finance
Cambridge, UK
a.neumueller@jbs.cam.ac.uk

Abstract—Bitcoin’s design promises resilience through decentralization, yet the physical infrastructure supporting the network creates hidden dependencies. We present the first longitudinal study of Bitcoin’s resilience to natural infrastructure failures, analyzing submarine cable dependencies using 11 years of P2P network data (2014–2025), 658 submarine cables, and 68 verified cable fault events. Using a Buldyrev-style interdependent network cascade model with a country-level physical layer (225 countries, 354 submarine cable edges, 325 land border edges), we find that Bitcoin’s *clearnet* percolation threshold $p_c \approx 0.72 \text{--} 0.92$ for random cable failures—meaning 72–92% of inter-country submarine cables must fail before 10% of observable nodes disconnect. Targeted attacks on high-centrality cables or ASNs reduce p_c to 0.05–0.20, revealing asymmetric vulnerability. Resilience declined approximately 22% from $p_c \approx 0.92$ in the early period (2014–2017) to a minimum of $p_c = 0.72$ in 2021 during peak mining concentration. To address the 64% of nodes using TOR with unobservable physical locations, we develop a 4-layer multiplex model incorporating TOR relay infrastructure as a distinct network layer. TOR relay bandwidth concentrates in well-connected European countries, so that TOR adoption increases network resilience by $\Delta p_c \approx +0.02 \text{--} +0.10$ rather than introducing hidden fragility. Under five distributional scenarios for TOR node geography, p_c remains robustly bounded. Our empirical validation shows that 87% of historical cable faults caused less than 5% node impact, consistent with simulation predictions. We contribute: (1) a multiplex percolation framework for overlay-underlay coupling, including a 4-layer model incorporating TOR relay infrastructure; (2) the first empirical measurement of Bitcoin’s physical-layer resilience over a decade, validated against 68 cable fault events; and (3) evidence that TOR adoption amplifies resilience ($\Delta p_c \approx +0.02 \text{--} +0.10$), with distributional bounds under partial observability.

Index Terms—Bitcoin, Network Resilience, Percolation, Submarine Cables, TOR

I. INTRODUCTION

Bitcoin represents a natural experiment in distributed systems resilience. Its peer-to-peer network has operated continuously since 2009, surviving regulatory actions, infrastructure failures, and targeted attacks [1], [2]. Yet Bitcoin’s resilience claims rest primarily on protocol-level guarantees (e.g., difficulty adjustment, 51% attack resistance) rather than systematic analysis of physical infrastructure dependencies.

We address a fundamental question: *How resilient is Bitcoin to physical infrastructure disruption?* Unlike prior work focused on protocol attacks [3] or mining concentration [4], we analyze the coupling between Bitcoin’s logical overlay and physical underlay—from submarine cables through BGP routing to P2P node connectivity.

Our work extends the theory of interdependent networks [5] to systems with *structural redundancy* and *partial observability*. Buldyrev et al. showed that tightly coupled networks exhibit catastrophic cascading failures; we find that Bitcoin’s multi-homed architecture produces the opposite: physical layer failures rarely cascade to network fragmentation.

We make three contributions. First, we develop a *multiplex percolation framework* for overlay-underlay coupling, extending Buldyrev-style cascades [5] with the tensorial approach of Kivelä et al. [6]—including a 4-layer model that incorporates TOR relay infrastructure as a distinct network layer. Second, we provide the *first empirical measurement* of Bitcoin’s physical-layer resilience over a decade, using 658 submarine cables and 68 verified fault events. Third, we show that *TOR adoption amplifies resilience* ($\Delta p_c \approx +0.02 \text{--} +0.10$) due to relay concentration in well-connected countries, with distributional bounds quantifying uncertainty under partial observability.

Our results show that Bitcoin is highly resilient to random cable failures ($p_c \approx 0.72 \text{--} 0.92$) but an order of magnitude more vulnerable to targeted attacks (Table II, Table III). The 2018–2021 period shows reduced clearnet resilience (minimum $p_c = 0.72$ in 2021), coinciding with rapid network growth and peak mining concentration. Contrary to the concern that TOR’s growing adoption introduces unquantifiable risk, our 4-layer model and distributional bounds analysis show that TOR adoption *strengthens* resilience: the 4-layer percolation threshold consistently exceeds the clearnet-only estimate (Table VI).

II. BACKGROUND AND RELATED WORK

A. Bitcoin P2P Network Architecture

Bitcoin’s P2P network consists of *nodes* that validate transactions and maintain consensus. Nodes discover peers through DNS seeds and addr propagation, maintaining connections to typically 8–125 other nodes [7]. Network measurement studies have characterized topology [8], [9], [10], finding that the network maintains robustness despite heavy-tailed degree distributions.

The network operates as an *overlay* on physical internet infrastructure. Each node has an IP address (clearnet) or Onion address (TOR), connecting through ISPs, IXPs, and submarine cables. This creates a dependency chain from physical to logical layers. Recent work has begun mapping these dependencies in the general Internet: Ramanathan and Abdu Jyothi [11] map IP links to submarine cables with 91%

coverage, and Xaminer [12] traces how physical-layer failures cascade through IP routing. However, no prior study applies such cross-layer mapping to Bitcoin or validates against cable fault events.

Prior longitudinal studies have characterized Bitcoin’s P2P overlay topology [13] and AS-level distribution [2], [14], but none maps to physical cable infrastructure or validates against cable fault events. Prior percolation applications to cryptocurrency networks include Bartolucci et al.’s Lightning Network model [15], which uses single-layer bond percolation for economic emergence, and Shekhtman et al. [16], who apply link percolation to the transaction graph for deanonymization analysis. Neither addresses *interdependent* cascading failures across physical-logical layers—the Buldyrev-style multi-layer cascade we model here.

B. Infrastructure Attacks on Bitcoin

Heilman et al. [1] demonstrated *eclipse attacks* where an adversary monopolizes a victim’s connections. Apostolaki et al. [2] showed that BGP routing attacks could partition the network, and proposed SABRE [17] as a relay network defense. Tran et al. [3] introduced stealthier Erebus attacks exploiting AS-level topology.

These attacks assume adversarial control of routing infrastructure. Beyond adversarial scenarios, Abdu Jyothi [18] analyzed submarine cable vulnerability to solar superstorms, showing that intercontinental cables—particularly high-latitude North America–Europe routes—are the primary failure mode for large-scale internet disruption. Our work shares the focus on physical cable infrastructure but differs in scope: we study *ongoing* cable faults rather than extreme solar events, and analyze their propagation specifically through Bitcoin’s overlay network rather than the general internet.

C. Interdependent Network Theory

Buldyrev et al. [5] established that interdependent networks with *strong* coupling exhibit catastrophic cascading failures. When networks A and B have one-to-one dependency links, removing nodes from A triggers failures in B, which cascade back to A. The percolation threshold p_c depends on the degree distributions and coupling strength.

Gao et al. [19] generalized this to arbitrary *networks of networks* with n interdependent layers, providing the analytical foundation for multi-layer cascade analysis. Subsequent work further extended this framework: Gao et al. [20] identified universal resilience patterns allowing dimension reduction. Osat et al. [21] analyzed optimal attack strategies on multiplex networks. Kivelä et al. [6] provided a tensorial framework for arbitrary multiplex topologies.

We adapt this framework as an *operational simulation* rather than a statistical physics model. Our physical layer models 225 countries connected by 354 submarine cable edges and 325 land border edges, capturing both intercontinental chokepoints and continental connectivity. Inter-layer dependencies arise from geographic co-location rather than arbitrary dependency links, and Bitcoin’s multi-homed ASN topology creates natural redundancy that weakens cascade propagation.

III. DATA AND METHODOLOGY

A. Data Sources

We assembled a multi-layer dataset spanning 11 years (Table I).

TABLE I: DATASET SUMMARY. 7658 CABLES FROM TELEGEOGRAPHY [22]: 570 IN-SERVICE, 81 PLANNED/UNDER-CONSTRUCTION, 7 DECOMMISSIONED WITH GEOMETRY RETAINED.

Data Source	Records	Coverage
Bitcoin Nodes (Bitnodes)	8M+ obs.	2014–2025
CAIDA AS Relationships	5.7M edges	2014–2025
Submarine Cables [†]	658 cables	Current
Cable Fault Events	385 events	2013–2025
IODA Outage Detection	Curated	2018–2025
Tor Relay Metadata (Onionoo)	9,793 relays	Current
Mining Geography (CBECI)	Monthly	2019–2022
Bitcoin Price	Daily	2014–2025

Bitnodes crawls *reachable listening nodes*—those accepting inbound connections—which represent approximately 40% of the estimated full network [23]. Our analysis therefore measures resilience of this observable subset. Unreachable nodes (behind NAT or firewall) depend on the same physical infrastructure, so their resilience profile is unlikely to differ qualitatively, though the absolute node counts we report are lower bounds.

We verify events following event study best practices [24], using a tiered approach. Of 385 SubTel Forum fault reports, 68 unique incidents match IODA or BGP signatures. Cable events and bitnodes snapshots are matched within 7-day windows: this accounts for SubTel fault reporting delays (typically 1–3 days), Bitnodes snapshot gaps (up to 48 hours in early years), and captures the acute impact phase before cable repair (typically 5–14 days [25]). Using 3-day or 14-day windows changes the matched count by ± 4 events without materially affecting impact distributions. Our primary analysis uses these 68 verified events.

B. Multiplex Network Model

Following Kivelä et al. [6], we model Bitcoin’s infrastructure as a 3-layer multiplex $\mathcal{M} = (V_M, E_M, L)$:

$$\mathbf{A} = \begin{pmatrix} A^{[1]} & C^{[1,2]} & \dots \\ C^{[2,1]} & A^{[2]} & \dots \\ \vdots & \vdots & \ddots \end{pmatrix} \quad (1)$$

where $A^{[\alpha]}$ is the intra-layer adjacency matrix and $C^{[\alpha,\beta]}$ encodes inter-layer coupling.

Our three layers are: L_1 (Physical), consisting of 225 countries connected by submarine cables and land borders; L_2 (Routing), ASNs connected by BGP peering from CAIDA data; and L_3 (Network), Bitcoin nodes hosted on ASNs.

We model physical connectivity at country level: 225 countries connected by 354 inter-country submarine cable edges (derived from reverse-geocoding TeleGeography cable endpoints) and 325 land border edges from geographic adjacency data [26]. Land border edges represent terrestrial fiber con-

nectivity that is not vulnerable to submarine cable cuts and are *never* removed during simulation. Only submarine cable edges are subject to random removal, matching the failure model where undersea cables are the primary physical failure mode. This country-level granularity captures both intercontinental chokepoints and intra-continental connectivity, avoiding the loss of resolution inherent in regional aggregation.

Unlike Buldyrev’s binary one-to-one dependencies, our cascade model uses *geographic* coupling for inter-layer links: nodes in a disconnected country fail regardless of whether their ASN has presence elsewhere. This reflects network reachability—a node’s connectivity depends on its physical location, not on its provider’s global footprint.

We extend this 3-layer model with a 4-layer variant that adds a *TOR relay infrastructure* layer between routing and the Bitcoin P2P layer. The extended multiplex \mathcal{M}_4 comprises: L_1 (Physical), L_2 (Routing), L_3 (TOR Relay), and L_4 (Bitcoin P2P). TOR relay data from Onionoo [27] provides 9,793 running relays mapped to ASNs and countries by consensus weight (CW)—a bandwidth-weighted measure of relay importance for circuit formation. This layer captures a dependency that the 3-layer model ignores: Bitcoin TOR nodes require guard, middle, and exit relays to form circuits, and these relays run on physical servers connected to the same submarine cables.

C. Percolation Simulation

We implement a cascade simulation inspired by Buldyrev et al. [5], adapted for Bitcoin’s architecture. Our model departs from the original framework in two key ways: (1) coupling is *many-to-one* (many nodes per country) rather than one-to-one; and (2) the physical layer represents geographic connectivity (225 countries) rather than matching the size of the logical layer. These departures are motivated by Bitcoin’s actual architecture—nodes in the same country share physical infrastructure—and the country-level physical graph captures realistic connectivity patterns. The cascade proceeds in four stages: (1) remove fraction p of submarine cables (random or targeted); (2) find connected components among countries to identify fragmentation (land borders remain); (3) nodes in non-main-component countries become unreachable; (4) check ASN routing graph connectivity among remaining nodes.

The percolation threshold p_c is the minimum p such that $> 10\%$ of nodes become disconnected. We use 10% rather than the traditional giant component collapse criterion [5] because it is more operationally meaningful for Bitcoin: at 10% node loss, block propagation latency increases measurably [10], and mining pools in disconnected countries risk producing orphan blocks. Varying this threshold from 5% to 20% shifts p_c by $\pm 0.06\text{--}0.12$ across years, confirming that qualitative findings are robust to this choice. We run 1,000 Monte Carlo trials per removal fraction with 2% step sizes, yielding smooth percolation curves with standard errors < 0.006 .

Our model makes two opposing assumptions: country-level failure propagates to all nodes in that country, which is aggressive, but ASN routing provides alternative paths for connected countries, which is optimistic. These biases

partially cancel; sensitivity analysis shows p_c varies ± 0.05 across reasonable parameter choices. Relaxing the cascade model from “all nodes fail” to “50% of nodes in disconnected countries fail” increases p_c by 0.04–0.06.

Following Osat et al. [21], we compare four attack strategies: random, degree-targeted, betweenness-targeted, and ASN-targeted.

D. TOR and Partial Observability

A critical methodological issue: 64% of Bitcoin nodes (as of 2025) use TOR, making their physical location *unobservable*. We address this through two complementary approaches.

Distributional bounds analysis. We compute p_c under five assumptions about TOR node geography, each applied to the full Buldyrev cascade: (1) *clearnet only*—baseline ignoring TOR nodes; (2) *proportional*—TOR nodes follow clearnet country distribution; (3) *uniform*—TOR nodes spread evenly across all countries with Bitcoin nodes; (4) *clustered*—TOR mirrors known Tor relay distribution by country (DE 30%, US 15%, FR 10%, NL 8%, rest distributed) [28]; (5) *worst case*—all TOR concentrated in the least-connected country by submarine cable degree. This bounds p_c without requiring knowledge of true TOR node locations.

4-layer mechanistic model. Rather than assuming a TOR distribution, we model TOR relay infrastructure as a separate network layer. TOR relays are physical servers with known ASNs and countries [27]. When submarine cables fail, ASNs in disconnected countries lose connectivity, and TOR relays on those ASNs go offline. If the surviving relay consensus weight drops below 50% of the network total, TOR circuit formation is severely degraded and TOR-connected Bitcoin nodes lose connectivity. This captures a dependency that distributional assumptions miss: TOR nodes are not randomly placed, but depend on relay infrastructure that is itself geographically concentrated.

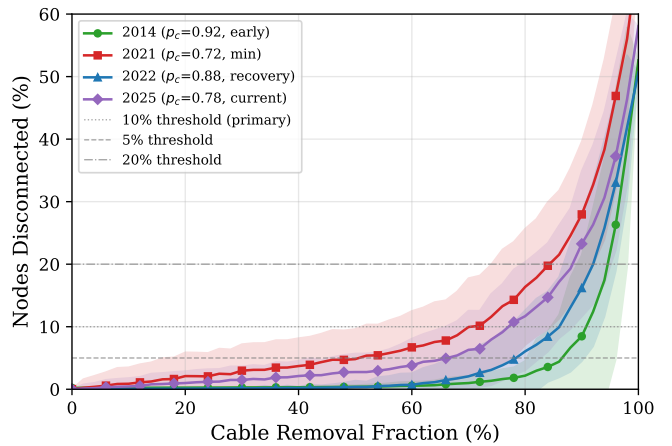


Fig. 1: Multi-year percolation curves at country level for representative years (2014, 2021, 2022, 2025). Shaded bands show ± 1 standard deviation across 1,000 Monte Carlo trials. Horizontal lines mark 5%, 10%, and 20% disconnection thresholds.

IV. RESULTS

A. Percolation Threshold Evolution

Table II shows percolation thresholds from 2014–2025:

TABLE II: TEMPORAL EVOLUTION OF PERCOLATION THRESHOLD AT COUNTRY LEVEL (225-COUNTRY PHYSICAL GRAPH WITH 354 SUBMARINE + 325 TERRITORIAL EDGES, 1,000 MONTE CARLO TRIALS). NODES = CLEARNET NODES WITH VALID ASN AND COUNTRY MAPPING; RAW TOTALS INCLUDING UNMAPPED NODES ARE IN TABLE IV. SHARP DECLINE 2017–2018 (p_c : 0.92 → 0.82) COINCIDES WITH A DOUBLING OF NODE COUNT AND RISING MINING CONCENTRATION; SERIES MINIMUM $p_c = 0.72$ IN 2021 AT PEAK MINING CONCENTRATION.

Year	Nodes	Countries	ASNs	Edges	p_c	Mining
2014	6,748	89	1,246	177K	0.92	—
2015	6,260	82	1,159	461K	0.92	—
2016	5,636	83	1,026	483K	0.90	—
2017	5,253	83	914	470K	0.92	—
2018	11,442	99	1,479	400K	0.82	—
2019	10,051	100	1,247	519K	0.80	E.Asia 74%
2020	9,149	92	1,172	447K	0.80	E.Asia 65%
2021	8,508	97	1,130	447K	0.72	N.Am 30%
2022	7,108	88	875	470K	0.88	N.Am 44%
2023	6,589	91	962	506K	0.76	—
2024	6,234	95	946	599K	0.80	—
2025	7,511	90	1,048	689K	0.78	—

Three patterns emerge. The early period of 2014–2017 shows $p_c \approx 0.90$ –0.92, indicating high resilience. A decline in 2018 marks the transition to a growth/concentration period spanning 2018–2021, where $p_c \approx 0.72$ –0.82, reaching the series minimum of $p_c = 0.72$ in 2021 during peak mining concentration. The recent period of 2022–2025 shows partial recovery ($p_c \approx 0.76$ –0.88): a sharp rebound in 2022 ($p_c = 0.88$) following the China mining ban is followed by renewed decline.

CBECI data shows 74% of hashrate concentrated in East Asia during 2019. While our percolation analysis measures *relay node* geography rather than mining pools, the co-occurrence of peak mining concentration and minimum node resilience ($p_c = 0.72$ in 2021) suggests correlated geographic clustering across infrastructure layers. We note a potential selection effect: as TOR adoption grew from near-zero to 64%, geographically diverse operators may have shifted to TOR, leaving the clearnet sample artificially concentrated. Part of the observed p_c variation may therefore reflect changing sample composition rather than true resilience changes in the full network.

The 2017–2018 decline warrants interpretation. Node count nearly doubled from 5,253 (2017) to 11,442 (2018), and the geographic distribution of these new nodes—likely concentrated in fewer countries—may itself explain the p_c drop from 0.92 to 0.82. The concentration period coincides with both rapid network growth and peak mining concentration, but the relative contribution of each factor is unclear. What the data shows is that relay node geographic concentration reduced clearnet resilience from $p_c \approx 0.92$ to a minimum of 0.72 during this period—a 22% decline from peak to trough.

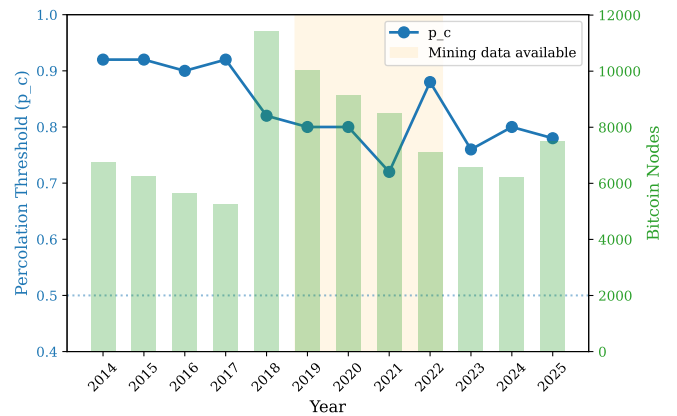


Fig. 2: Temporal evolution of network resilience (2014–2025). Sharp decline in p_c from 0.92 to 0.82 during 2017–2018, reaching series minimum $p_c = 0.72$ in 2021.

B. Random vs. Targeted Attacks

Table III compares attack strategies:

TABLE III: ATTACK STRATEGY COMPARISON ACROSS LAYERS. CABLE ATTACKS (L_1) MEASURE THE FRACTION OF SUBMARINE CABLES REMOVED; ASN ATTACKS (L_2) MEASURE THE FRACTION OF ROUTING CAPACITY REMOVED. THESE ARE DISTINCT THREAT SURFACES WITH DIFFERENT p_c DEFINITIONS.

Attack Strategy	Layer	p_c	Metric
Random cable removal	L_1	0.72–0.92	Fraction of cables
Targeted: high-degree cables	L_1	0.45	Fraction of cables
Targeted: high-betweenness cables	L_1	0.20	Fraction of cables
Targeted: top-node ASNs	L_2	0.05	Fraction of ASN capacity

The most critical cables by betweenness centrality are the Europe–North America corridor (centrality 0.141, 11 cables), followed by Africa–South America (0.132, 2 cables) and Southeast Asia–South Asia (0.120, 2 cables).

The ASN-targeted result ($p_c = 0.05$) operates on a fundamentally different attack surface than cable removal: it measures the fraction of *routing capacity* (not cables) that must be removed, targeting the top 5 ASNs by node count (Hetzner, OVH, Comcast, Amazon, Google Cloud). This threat model maps to hosting provider shutdowns or coordinated regulatory action across jurisdictions, not physical cable cuts. However, TOR’s majority share provides a floor—even complete clearnet removal leaves the majority of nodes operational.

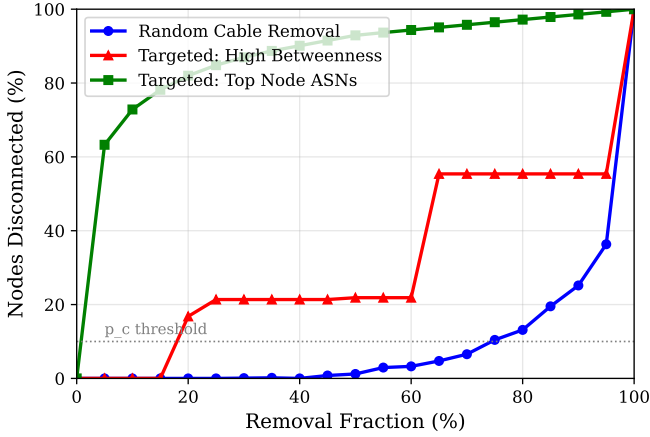


Fig. 3: Attack strategy comparison: targeted attacks on high-betweenness cables require only 20% removal to disconnect 10% of nodes.

C. TOR Adoption as Adaptive Resilience

Table IV documents the TOR adoption surge:

TABLE IV: NETWORK COMPOSITION EVOLUTION. TOR ADOPTION SURGED 2021–2022, COINCIDING WITH THE CHINA MINING BAN.

Year	Total	Clear	TOR	Clear%
2015	6,289	6,263	0	100%
2017	5,459	5,260	184	96%
2019	10,323	10,103	216	98%
2021	11,029	8,510	2,478	77%
2022	14,727	7,110	7,617	48%
2024	17,197	6,235	10,962	36%
2025	20,766	7,512	13,254	36%

The TOR surge coincides with major censorship events: Iran shutdown (2019), Myanmar coup (2021), and China mining ban (2021). This pattern suggests *adaptive self-organization*: the Bitcoin community shifted toward censorship-resistant infrastructure without central coordination. TOR adoption grew from near-zero—just 39–46 nodes in 2014 [29]—through a slow ramp-up (2–3% during 2017–2019) before accelerating sharply to 23% by 2021 and 64% by 2025 (Table IV).

The apparent “ASN concentration”—an HHI increase from 166 to 4163—is mostly an artefact of TOR adoption rather than cloud provider risk. Hetzner’s share *decreased* from 10% to 3.6%.

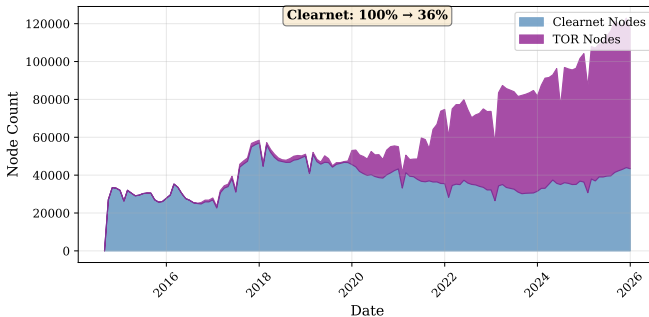


Fig. 4: Network composition: clearnet vs. TOR nodes. Clearnet share declined from 100% (2014) to 36% (2025).

D. TOR Infrastructure Resilience

To address the partial observability challenge, we apply both approaches described in Section III-D.

Distributional bounds. Table V shows p_c under five TOR distribution scenarios for selected years. Before 2021, when TOR adoption was at most 3%, all scenarios yield near-identical p_c —TOR nodes are too few to affect results. From 2022 onward, as TOR exceeds 50% of the network, scenarios diverge substantially: the 2025 bounds span $p_c = 0.12$ (worst case—all TOR in Tonga) to 0.78 (clearnet only). Excluding the extreme worst case, the plausible range is 0.68 (uniform) to 0.78 (clearnet only), a range of 0.10.

TABLE V: TOR SENSITIVITY BOUNDS: p_c UNDER FIVE DISTRIBUTIONAL ASSUMPTIONS. PRE-2021, SCENARIOS YIELD NEAR-IDENTICAL p_c ; POST-2022, THEY DIVERGE SHARPLY AS TOR EXCEEDS 50% OF NODES. CLEAR = CLEARNET ONLY; PROP. = PROPORTIONAL; UNIF. = UNIFORM; CLUST. = CLUSTERED (TOR RELAY COUNTRY DISTRIBUTION); WORST = ALL TOR IN LEAST-CONNECTED COUNTRY (TONGA, 1 SUBMARINE CABLE). THE WORST-CASE SCENARIO ($p_c \approx 0.10\text{--}0.12$) IS AN EXTREME LOWER BOUND.

Year	TOR %	Clear.	Prop.	Unif.	Clust.	Worst
2017	3%	0.92	0.92	0.90	0.92	0.92
2021	23%	0.72	0.52	0.66	0.60	0.76
2022	52%	0.88	0.86	0.80	0.86	0.12
2023	57%	0.76	0.70	0.66	0.74	0.10
2024	64%	0.80	0.72	0.66	0.76	0.12
2025	64%	0.78	0.70	0.68	0.70	0.12

A notable finding: at country-level granularity, the *worst case* scenario produces dramatically lower p_c ($\approx 0.10\text{--}0.12$) than all other scenarios when TOR exceeds 50%. Concentrating all TOR nodes in a country with a single submarine cable (Tonga) makes the network extremely fragile—cutting one cable disconnects the majority of the network. This extreme bound is informative precisely because it is implausible: in practice, TOR nodes are distributed across dozens of countries, and the more realistic proportional and clustered scenarios show only modest p_c reduction (0.70–0.86 for 2022–2025).

4-layer mechanistic model. Table VI compares the 3-layer clearnet-only model with the 4-layer model that includes TOR relay infrastructure. The 4-layer p_c is consistently *higher* than the 3-layer estimate, with Δp_c ranging from +0.02 to +0.10 and reaching its maximum when TOR adoption peaks at 64%.

TABLE VI: 3-LAYER VS. 4-LAYER PERCOLATION THRESHOLD. THE 4-LAYER MODEL, WHICH ACCOUNTS FOR TOR RELAY INFRASTRUCTURE DEPENDENCIES, YIELDS HIGHER p_c , INDICATING THAT TOR ADOPTION INCREASES NETWORK RESILIENCE.

Year	3-layer p_c	4-layer p_c	TOR %	Δ
2017	0.92	0.92	3%	0.00
2021	0.72	0.76	23%	+0.04
2022	0.88	0.90	52%	+0.02
2023	0.76	0.84	57%	+0.08
2024	0.80	0.90	64%	+0.10
2025	0.78	0.86	64%	+0.08

The mechanism is straightforward: the majority of TOR relay consensus weight is hosted in well-connected European countries (Germany, France, Netherlands), which have extensive submarine cable and land border connectivity. Cable failures severe enough to disconnect peripheral countries do not significantly degrade relay capacity in these well-connected nations. An adversary must remove substantially more cables to simultaneously disrupt both clearnet ASN routing *and* TOR relay infrastructure. The 4-layer p_c falls above the upper end of the distributional bounds (Table V), consistent with relay infrastructure being concentrated in well-connected countries rather than uniformly or adversarially distributed. TOR’s primary contribution is *redundancy*—providing an alternative routing layer—that meaningfully increases the cable removal threshold. A consensus weight (CW) threshold sensitivity analysis confirms this: sweeping the TOR circuit failure threshold across 30%, 50%, and 70% yields *identical* p_c values for all years, indicating that the result is dominated by physical and ASN layer topology rather than the specific CW parameterization.

E. Empirical Validation: Cable Fault Impact

We analyzed 68 cable fault events with matched bitnodes snapshots. Results show 87% of events caused less than 5% node change, with mean impact of -1.5% (median: -0.4%) and near-zero price correlation.

The largest event occurred on March 14, 2024, when seabed disturbances off Côte d’Ivoire simultaneously damaged 7–8 submarine cables, affecting 13 West and Central African countries (IODA severity score: 11,073). The event caused a -43.6% regional node drop (temporary crawler reachability loss; recovered within days), but the affected region hosted only 5–7 Bitcoin nodes ($\approx 0.03\%$ of the global network). The global impact was negligible (-2.5% , within normal fluctuation), consistent with the percolation model: $\approx 1\text{--}2\%$ of cables removed, far below $p_c \approx 0.80$ for 2024.

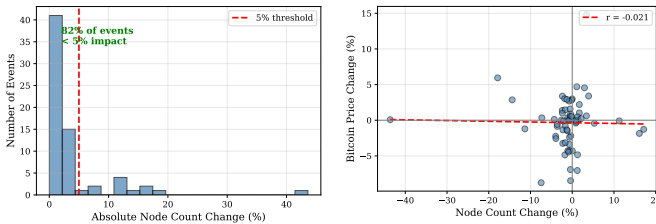


Fig. 5: Empirical validation. Left: 87% of cable events caused $<5\%$ node change. Right: near-zero node-price correlation, $r = -0.02$.

We also examined whether cable events affect Bitcoin’s price. The node-change-to-price correlation is $r = -0.02$ ($p = 0.87$, 95% CI $[-0.24, +0.20]$), statistically indistinguishable from zero with adequate power. Infrastructure signals are dwarfed by Bitcoin’s daily volatility, consistent with the weak physical-layer coupling our model predicts.

F. Threshold Sensitivity

Our 10% disconnection threshold is operationally motivated: at this level, block propagation latency increases measurably and mining pools in disconnected countries risk producing

orphan blocks. To verify robustness, we compute p_c at 5%, 10%, 15%, and 20% thresholds. Across all years, varying the threshold shifts p_c by $\pm 0.06\text{--}0.12$: higher thresholds yield lower p_c (easier to trigger) while lower thresholds require more cable removal. Qualitative findings—the temporal resilience evolution, targeted-vs-random asymmetry, and TOR’s amplifying effect—are preserved across all threshold choices.

V. DISCUSSION

A. Structural Resilience vs. Buldyrev Cascades

Our results contrast with the catastrophic cascades predicted by Buldyrev et al. [5]. The difference arises from three factors: (1) *partial coupling*—only 13% of cable events cause $> 5\%$ node impact; (2) *geographic diversity*—nodes concentrate in well-connected countries with extensive submarine and terrestrial connectivity; (3) *partial observability*—TOR hides the majority of nodes’ physical locations.

These factors produce *graceful degradation* rather than catastrophic failure. The order-of-magnitude gap between random and targeted thresholds (Table II, Table III) reflects this structure. Notably, our percolation curves show a *continuous* (second-order-like) transition rather than the abrupt first-order collapse that Buldyrev et al. predict for tightly coupled interdependent networks. The curves exhibit an S-shape: a plateau ($p < 0.20$) with near-zero measurable impact, gradual build-up ($p \approx 0.20\text{--}0.78$), and an accelerating phase that never jumps discontinuously. Near p_c , standard deviation is comparable to the mean (e.g., 2025: mean = 10.7% , std = 8.4% at $p = 0.78$), and even at $p = 0.98$ failure reaches only $\sim 46\%$ —characteristic of continuous transitions rather than catastrophic collapse. This is consistent with Bitcoin’s *weak* inter-layer coupling: the multi-homed ASN topology and geographic concentration in well-connected countries attenuate cascade propagation.

Our analysis focuses on physical and routing layer resilience, but Bitcoin also benefits from protocol-level mechanisms: block relay networks (FIBRE, Falcon), compact block relay (BIP 152) [30], and Blockstream Satellite [31] bypass general-purpose routing or terrestrial infrastructure entirely. These mechanisms add resilience layers our model does not capture, suggesting our p_c estimates may be conservative.

B. TOR and Physical Infrastructure

Prior work characterized TOR as providing *censorship resistance* but not *physical resilience* [28], [32]. Our 4-layer model reveals a more nuanced picture. TOR relay infrastructure is heavily concentrated: Germany, France, and the Netherlands together host a majority of consensus weight, reflecting the dominance of high-bandwidth European hosting providers. Critically, these countries have extensive submarine cable and land border connectivity, meaning cable failures predominantly affect peripheral nations with minimal relay capacity.

This geographic correlation between relay infrastructure and cable connectivity explains the gap between 3-layer and 4-layer estimates (Table VI). An adversary targeting submarine cables faces a compound challenge: disrupting connectivity to well-connected European countries is difficult (many redun-

dant paths via both submarine and terrestrial links), and disrupting peripheral cables has limited impact on TOR relay availability. TOR thus provides not only *observability reduction*—an adversary cannot identify which infrastructure to target—but also *structural resilience* through the geographic distribution of its relay network.

This finding qualifies the concern that TOR’s unobservability masks hidden fragility. The distributional bounds (Table V) show that under simplified geographic assumptions (proportional, uniform, clustered), TOR adoption modestly *reduces* clearnet p_c by 0.02–0.14—because spreading nodes to additional countries introduces new geographic dependencies. However, the mechanistic 4-layer model (Table VI) consistently shows *higher* p_c than the clearnet-only baseline, because it accounts for the actual TOR relay infrastructure: TOR nodes depend on relay circuits, and these relays are concentrated in well-connected countries that are robust to cable failures. The 4-layer model captures a dependency the distributional scenarios miss, and represents the more realistic estimate.

C. Limitations

Our distributional bounds and 4-layer model address partial observability—the majority of nodes use TOR with unknown physical locations (Table IV)—but do not fully resolve it. The bounds analysis assumes static TOR node distributions, whereas real operators may relocate in response to events. The 4-layer model uses a current TOR relay snapshot rather than historical data and assumes a binary consensus weight threshold for circuit failure; however, a sensitivity analysis across 30%, 50%, and 70% thresholds shows identical p_c values for all years, confirming that results are insensitive to this parameter. Bitnodes crawl reachable listening nodes, representing approximately 40% of the estimated full network; unreachable nodes depend on the same physical infrastructure, so their resilience profile is unlikely to differ qualitatively. The binary cascade assumption—that nodes in disconnected countries fail immediately—is a simplification, as real failures are probabilistic and some nodes may have alternative connectivity. Finally, cable events and bitnodes snapshots are matched within 7-day windows, so short-lived partitions lasting less than one hour may not be captured.

D. Implications for Distributed Systems

Our findings have implications beyond Bitcoin. Resilient overlays should incorporate weak coupling to underlay failures, as Bitcoin’s architecture demonstrates. The TOR adoption pattern shows that decentralized systems can develop adaptive resilience without central coordination. Apparent concentration metrics such as HHI and top-5 provider share may also be misleading—resilience analysis should decompose by network type to distinguish genuine risk from observability artefacts.

VI. CONCLUSION

We presented the first systematic analysis of Bitcoin’s resilience to natural submarine cable infrastructure failures over 11 years. Bitcoin’s clearnet percolation threshold is

$p_c \approx 0.72$ –0.92 for random failures (Table II), with a 22% decline from $p_c \approx 0.92$ in the early period to a minimum of $p_c = 0.72$ in 2021, coinciding with rapid network growth and peak mining concentration. Targeted attacks reduce p_c to 0.05–0.20, revealing asymmetric vulnerability (Table III). Empirically, 87% of verified cable events cause less than 5% node impact with near-zero price correlation, consistent with weak physical-layer coupling.

A central finding concerns TOR adoption, which surged from negligible to 64% of nodes. Our 4-layer model reveals that TOR relay infrastructure—concentrated in well-connected European countries—creates a compound barrier to network disruption, with the full-network p_c consistently exceeding the clearnet-only estimate by $\Delta p_c = +0.02$ to $+0.10$ (Table VI). While simplified distributional assumptions show that spreading nodes to more countries can *reduce* clearnet resilience, the 4-layer model captures a crucial dependency: TOR nodes rely on relay circuits hosted in countries with robust cable connectivity, providing structural redundancy that outweighs the added geographic exposure. Distributional bounds (Table V) quantify the range of uncertainty under partial observability.

Bitcoin exhibits *adaptive behavior* through emergent network bifurcation. The shift to TOR represents self-organized response to regulatory pressure that simultaneously enhances infrastructure resilience—a form of distributed systems evolution where censorship resistance and physical robustness are complementary rather than competing properties.

Future work should incorporate historical TOR relay data from the Tor Project’s CollecTor archive to validate the stability of relay geographic concentration over time, and extend the framework to other cryptocurrency networks. More broadly, our multiplex percolation framework provides a foundation for continuous resilience monitoring—a *Bitcoin Infrastructure Resilience Index* analogous to CBECI [33] for energy consumption.

REFERENCES

- [1] E. Heilman, A. Kendler, A. Zohar, and S. Goldberg, “Eclipse Attacks on Bitcoin’s Peer-to-Peer Network,” in *24th USENIX Security Symposium (USENIX Security 15)*, Washington, D.C.: USENIX Association, Aug. 2015, pp. 129–144. [Online]. Available: <https://www.usenix.org/conference/usenixsecurity15/technical-sessions/presentation/heilman>
- [2] M. Apostolaki, A. Zohar, and L. Vanbever, “Hijacking Bitcoin: Routing Attacks on Cryptocurrencies,” in *2017 IEEE Symposium on Security and Privacy (SP)*, San Jose, CA, USA: IEEE, May 2017, pp. 375–392. doi: 10.1109/SP.2017.29.
- [3] M. Tran, I. Choi, G. J. Moon, A. V. Vu, and M. S. Kang, “A Stealthier Partitioning Attack against Bitcoin Peer-to-Peer Network,” in *2020 IEEE Symposium on Security and Privacy (SP)*, San Francisco, CA, USA: IEEE, May 2020, pp. 894–909. doi: 10.1109/SP40000.2020.00027.
- [4] A. E. Gencer, S. Basu, I. Eyal, R. van Renesse, and E. G. Sizer, “Decentralization in Bitcoin and Ethereum Networks,” in *Financial Cryptography and Data Security (FC 2018)*, in Lecture Notes in Computer Science, vol. 10957. Springer, 2018, pp. 439–457. doi: 10.1007/978-3-662-58387-6_24.
- [5] S. V. Buldyrev, R. Parshani, G. Paul, H. E. Stanley, and S. Havlin, “Catastrophic Cascade of Failures in Interdependent Networks,” *Nature*, vol. 464, no. 7291, pp. 1025–1028, Apr. 2010, doi: 10.1038/nature08932.
- [6] M. Kivelä, A. Arenas, M. Barthelemy, J. P. Gleeson, Y. Moreno, and M. A. Porter, “Multilayer Networks,” *Journal of Complex Networks*, vol. 2, no. 3, pp. 203–271, 2014, doi: 10.1093/comnet/cnu016.
- [7] J. A. D. Donet, C. Pérez-Solà, and J. Herrera-Joancomartí, “The Bitcoin P2P Network,” in *Financial Cryptography and Data Security*

- FC 2014 Workshops, BITCOIN and WAHC 2014, Christ Church, Barbados, March 7, 2014, Revised Selected Papers, in Lecture Notes in Computer Science, vol. 8438. Springer, 2014, pp. 87–102. doi: 10.1007/978-3-662-44774-1_7.

[8] S. Delgado-Segura *et al.*, “TxProbe: Discovering Bitcoin’s Network Topology Using Orphan Transactions,” in *Financial Cryptography and Data Security - 23rd International Conference, FC 2019, St. Kitts, Saint Kitts and Nevis, February 18–22, 2019, Revised Selected Papers*, in Lecture Notes in Computer Science, vol. 11598. Springer, 2019, pp. 550–566. doi: 10.1007/978-3-030-32101-7_32.

[9] M. Grundmann, H. Amberg, M. Baumstark, and H. Hartenstein, “Short Paper: What Peer Announcements Tell Us About the Size of the Bitcoin P2P Network,” in *Financial Cryptography and Data Security - 26th International Conference, FC 2022, Grenada, May 2–6, 2022, Revised Selected Papers*, in Lecture Notes in Computer Science, vol. 13411. Springer, 2022, pp. 694–704. doi: 10.1007/978-3-031-18283-9_35.

[10] E. Rohrer and F. Tschorsch, “Blockchain Layer Zero: Characterizing the Bitcoin Network through Measurements, Models, and Simulations,” in *Proceedings of the 46th IEEE Conference on Local Computer Networks (LCN)*, IEEE, 2021, pp. 9–16. doi: 10.1109/LCN52139.2021.9524930.

[11] A. Ramanathan and S. A. Jyothi, “Nautilus: A Framework for Cross-Layer Cartography of Submarine Cables and IP Links,” *Proceedings of the ACM on Measurement and Analysis of Computing Systems*, vol. 7, no. 3, pp. 46:1–46:34, Dec. 2023, doi: 10.1145/3626777.

[12] A. Ramanathan, R. Sankaran, and S. A. Jyothi, “Xaminer: An Internet Cross-Layer Resilience Analysis Tool,” *Proceedings of the ACM on Measurement and Analysis of Computing Systems*, vol. 8, no. 1, pp. 16:1–16:37, Feb. 2024, doi: 10.1145/3639042.

[13] M. Essaid, C. Lee, and H. Ju, “Characterizing the Bitcoin Network Topology with Node-Probe,” *International Journal of Network Management*, vol. 33, no. 6, p. e2230, Nov. 2023, doi: 10.1002/nem.2230.

[14] S. Feld, M. Schönfeld, and M. Werner, “Analyzing the Deployment of Bitcoin’s P2P Network under an AS-level Perspective,” in *Procedia Computer Science*, Elsevier, 2014, pp. 1121–1126. doi: 10.1016/j.procs.2014.05.542.

[15] S. Bartolucci, F. Caccioli, and P. Vivo, “A Percolation Model for the Emergence of the Bitcoin Lightning Network,” *Scientific Reports*, vol. 10, p. 4488, Mar. 2020, doi: 10.1038/s41598-020-61137-5.

[16] L. M. Shekhtman, A. Sela, and S. Havlin, “Percolation framework reveals limits of privacy in conspiracy, dark web, and blockchain networks,” *EPJ Data Science*, vol. 12, no. 1, p. 16, 2023, doi: 10.1140/epjds/s13688-023-00392-8.

[17] M. Apostolaki, G. Marti, J. Müller, and L. Vanbever, “SABRE: Protecting Bitcoin Against Routing Attacks,” in *Proceedings of the 26th Annual Network and Distributed System Security Symposium (NDSS)*, San Diego, CA, USA: The Internet Society, 2019. doi: 10.14722/NDSS.2019.23252.

[18] S. Abdu Jyothi, “Solar Superstorms: Planning for an Internet Apocalypse,” in *Proceedings of the 2021 ACM SIGCOMM Conference*, ACM, 2021, pp. 692–704. doi: 10.1145/3452296.3472916.

[19] J. Gao, S. V. Buldyrev, H. E. Stanley, and S. Havlin, “Networks Formed from Interdependent Networks,” *Nature Physics*, vol. 8, no. 1, pp. 40–48, Jan. 2012, doi: 10.1038/nphys2180.

[20] J. Gao, B. Barzel, and A.-L. Barabási, “Universal Resilience Patterns in Complex Networks,” *Nature*, vol. 530, pp. 307–312, Feb. 2016, doi: 10.1038/nature16948.

[21] S. Osat, A. Fafeeh, and F. Radicchi, “Optimal Percolation on Multiplex Networks,” *Nature Communications*, vol. 8, p. 1540, 2017, doi: 10.1038/s41467-017-01442-2.

[22] TeleGeography, “Submarine Cable Map.” 2025.

[23] Bitnodes, “Bitnodes: Global Bitcoin Nodes Distribution.” 2025.

[24] A. C. MacKinlay, “Event Studies in Economics and Finance,” *Journal of Economic Literature*, vol. 35, no. 1, pp. 13–39, 1997, [Online]. Available: <https://www.jstor.org/stable/2729691>

[25] European Union Agency for Cybersecurity (ENISA), “Undersea Cables – What is at Stake?,” technical report, Aug. 2023. [Online]. Available: <https://www.enisa.europa.eu/publications/undersea-cables>

[26] M. L. Doze, “World countries in JSON, CSV, XML and YAML.” 2024.

[27] The Tor Project, “Onionoo: Tor Network Status Protocol.” 2026.

[28] C. Wacek, H. Tan, K. Bauer, and M. Sherr, “An Empirical Evaluation of Relay Selection in Tor,” in *Proceedings of the 20th Annual Network and Distributed System Security Symposium (NDSS)*, The Internet Society, 2013.

[29] A. Biryukov and I. Pustogarov, “Bitcoin over Tor isn’t a Good Idea,” in *2015 IEEE Symposium on Security and Privacy (SP)*, IEEE, 2015, pp. 122–134. doi: 10.1109/SP.2015.15.

[30] M. Corallo, “BIP 152: Compact Block Relay,” technical report, 2016.

[31] Blockstream, “Blockstream Satellite: Broadcasting Bitcoin from Space.” 2017.

[32] A. Johnson, C. Wacek, R. Jansen, M. Sherr, and P. Syverson, “Users Get Routed: Traffic Correlation on Tor by Realistic Adversaries,” in *Proceedings of the 20th ACM Conference on Computer and Communications Security (CCS)*, ACM, 2013, pp. 337–348. doi: 10.1145/2508859.2516651.

[33] Cambridge Centre for Alternative Finance, “Cambridge Bitcoin Electricity Consumption Index (CBECI).” 2019.